Visual Geometry Group based on U-Shaped Model for Liver Tumor Segmentation

Javaria Amin, Muhammad Almas Anjum, Muhammad Sharif, Seifedine Kadry, Ruben González Crespo

***Abstract*— Liver cancer is the primary reason of death around the globe. Manually detecting the infected tissues is a challenging and time-consuming task. The computerized methods help make accurate decisions and therapy processes. The segmentation accuracy might be increased to reduce the loss rate. Semantic segmentation performs a vital role in infected liver region segmentation. This article proposes a method that consists of two major steps; first, the local Laplacian filter is applied to improve the image quality. The second is the proposed semantic segmentation model in which features are extracted to the pre-trained VGG16 model and passed to the U-shaped network. This model consists of 51 layers: input, 23 convolutional, 4 max pooling, 4 transpose convolutional, 4 concatenated, 8 activation, and 7 batch-normalization. The proposed segmentation framework is trained on the selected hyperparameters that reduce the loss rate and increase the segmentation accuracy. The proposed approach more precisely segments the infected liver region. The proposed approach performance is accessed on two datasets such as 3DIRCADB and LiTS17. The proposed framework provides an average dice score of 0.98, which is far better compared to the existing works.**

***Index Terms*— Convolutional Neural Network, Segmentation, Datasets, Liver.**

I. Introduction

The liver regularly purifies the blood that flows through the body, transforming substances ingested through the digestive tract into chemicals ready for use. Other crucial tasks carried out by the liver include clearing poisons and harmful chemical products in blood and preparing them for disposal. The liver is particularly susceptible to cancer cells moving through the bloodstream since it is the organ through which all blood in the body passes. Primary liver cancer, which develops in the liver, and cancer that begins in further regions of the body and extent to the liver, can both impact the liver [1, 2].

Javaria Amin is with the Department of Computer Science, University of Wah, Wah Cantt, Pakistan (Javeria.amin@uow.edu.pk), Muhammad Almas Anjum is with National University of Technology (NUTECH), Islamabad, Pakistan (almasanjum@yahoo.com), Muhammad Sharif is with Department of Computer Science, COMSATS University Islamabad, Wah Cantt, Pakistan (sharif@ciitwah.edu.pk), Seifedine Kadry is with the department of applied data science, Noroff University College, Norway, Artificial Intelligence Research Center (AIRC), Ajman University, Ajman, 346, United Arab Emirates, and Department of Electrical and Computer Engineering, Lebanese American University, Byblos, Lebanon (skadry@gmail.com), Ruben González Crespo is with Department of Computer Science, Universidad Internacional de La Rioja, Logroño, La Rioja, Spain (ruben.gonzalez@unir.net).

A significant number of people worldwide die from liver cancer each year. It is a notably prevalent cancer. Early identification, diagnosis, and treatment are essential to increase the survival chance and overall quality of life for individuals with liver cancer. Computed tomography (CT), which has a good signal-to-noise ratio, excellent spatial resolution, rapid scanning speed, and a relatively inexpensive cost, is frequently utilized in clinical practice to detect hepatic malignancy [3]. For disease diagnosis and therapy planning, segmented liver tumor pixels using CT scans is a crucial and critical stage. It can offer exact details, such as the shape, and location size of tumors, to assist clinicians in selecting the best course of therapy. But segmentation is often carried out manually by skilled radiologists, which is time-consuming and exhausting. Therefore, there is a critical need for and growing interest in developing automatic or semi-automatic systems for segmenting liver tumors. Because of variations in the anatomical structure of the tumor, shape, and size (1), (2) irregular boundaries among surrounding liver tissues, and the tumor (3) noise appearance caused through CT, robust and accurate tumor segmentation is still a challenge. Only low-level visual characteristics, such as gradient, intensity, and texture, which can be directly deduced from the image, are used to accomplish segmentation through image-based algorithms, which primarily include thresholding, region growth, and clustering. These techniques readily result in the leakage of boundaries on ambiguous boundaries because of the minimal information used. Some model-based approaches, such as level sets and graph cuts, use the information of low and high-level to increase the accuracy. The techniques often succeed in producing appropriate segmentations for tumors with homogenous intensities and solid borders, but they fall short with appearance variability and poor contrast.

Furthermore, the model and image techniques might not provide fully automated segmentation because of a lack of prior knowledge [4]. Therefore, the attention scale model is utilized for the segmentation, giving a dice score of 0.844 [5]. The three-dimensional U-net is used for segmentation with a 0.59 F1 score [6]. The liver region is extracted using 3D-Unet and divided the region of liver into similar superpixels through the LI-SLIC method. It recursively decomposed superpixels based on the intensity and boundaries of the tumor pixels.

Moreover, SVM is used to classify the normal/abnormal slices based on texture and intensity features [7]. Adaptive histogram equalization improves the image quality, and Otsu is used to segment the liver tumor using ultrasound images with

0.99 accuracy [8]. The pre-trained ResNet is used behind the U-net for segmentation. This method is evaluated on the IRCADB01 dataset and gives 0.99 accuracy [9]. The four-dimensional DL model with LSTM for lesion segmentation with 0.82 dice score [10]. The edge-based localization model is applied to localize the tumor region. This model performance is evaluated on the local dataset that contains 215 subjects and provides 0.90 accuracy [11]. In literature, much work is done for segmentation. However, there is still a gap in this domain because liver images of CT are complex, where contrast among tissues and organs is low, and feature extraction is a challenging task [12]. Therefore, it is essential to adopt a technique carried out to model global spatial information effectively and efficiently [44][45] [46] [47]. In this research attenuation-based, U-network is proposed, which is trained on the selected learning parameters for segmentation.

- A visual geometry group based on a U-Shaped model is proposed for the segmentation. The proposed segmentation framework is trained on the selected hyperparameters that significantly reduce the loss rate and increase the segmentation accuracy.
- The proposed segmentation model results are also compared to the traditional semantic segmentation models such as FCN, SegNet, and U-network. The experimental investigation reveals that the results are far better than those of traditional segmentation models.

II. RELATED WORKS

The cascaded model is developed for the segmentation. This method fuses features at distinct levels and combines with the attention method to concentrate the significant information. The spatial atrous pyramid attention pooling block is utilized to extract multiple features. These features are fused fully at every network layer. The results are computed on 3DIRCADb and LiTS datasets with a 0.81 dice score [13-16]. The pyramid-decoupled correlation model is used for segmentation. This model performance is accessed on the MICCAI-2017 dataset, giving dice of 0.76 [17]. The scale attention axis (SAA) model is proposed for segmentation, and results are computed on the LiTS2017 dataset that provides a 0.84 dice score [5]. The u-network is modified skip pathways based on locally reconstructed features and fusion of the features representing contextual detailed high-level features information for tumor segmentation [18, 19]. The results are evaluated on 3DIRCADb and LiTS datasets with average dice score of 0.77 [20]. The residual path is added in activation and deconvolution operations. The skip connection is avoided where low-resolution feature information is duplicated in U-net. Therefore, an improved U-net is suggested for segmentation using the LiTS-2017 dataset that provided a DSC of 0.89 [21]. FCN model is modified for segmentation based on CT images and the results are computed on JDRD and 3Dircadb datasets that provided VOE of 8.1 ± 4.5 and 15.6 ± 4.3, respectively [22]. The hybrid densely U-network is proposed for segmentation that consists of a three-dimensional counterpart for aggregating hierarchically volumetric features and performing end-to-end learning. The results of this method are computed on 3DIRCADb and MICCAI-1017 datasets [23]. The deeplabv3 is used for segmentation in which the Pix2pix model is used as the generation of the adversarial. This model is trained on the multi-scale cross-entropy loss that provided a 0.97 dice score at the testing phase [24]. The deep network with the addition of dense-Unet and pyramid mapping of the features is used for the segmentation [25]. The two-dimensional E^2-Network is designed for segmentation [26]. The handcrafted contextual, range and variance features are extracted from CT liver slices and fed to the SVM, random forest, and AdaBoost, which provided 80.06% ± 1.63% dice score, 82.67% ± 1.43% precision, and recall of 84.34% ± 1.61% [27]. The deep hybrid model is used for segmentation using CT images, and results are computed on 3D-IRCADb and LiTS datasets that give 0.94 and 0.73 dice score [28]. The hybrid attention connection model is designed by combining hard and soft attention and short/long connections of the skip. The cascaded model is also used with improved loss function for more accurate segmentation of the infected liver region. The results are computed on two datasets, such as 3DIRCADb, with a dice score of 0.95 liver/0.73 tumor [29]. Watershed and graph-cut methods are used for segmentation [30]. The two-dimensional U-network is used with a random forest for segmentation [31]. The U^3 and U^2 networks are used for segmentation. The results are computed on 3DIRCADb and LiTS datasets that provided liver/tumor with 0.964/0.733 and 0.963/0.736 dice score [32].

The most recent related works have a gap to improve the results in terms of accuracy and dice score. Some methods only calculate the accuracy while dice score is also an important measure that is not computed. Few articles computed accuracy and dice score but these results can also be improved by proposing new method. Therefore, the method is proposed for segmentation of liver that consists of Local Laplacian Filter to improve the image quality and Vgg-16 is used with U-net which is trained on the selected hyperparameters to segment the tumor more accurately.

III. PROPOSED METHODOLOGY

The semantic segmentation architecture is designed for segmentation using CT images as illustrated in Figure 1. In the proposed segmentation model features are derived from the pre-trained VGG-16 model and provided as input to the U-shaped model that consists of 51 layers. The proposed model is trained on the selected hyperparameters such as sgdm optimizer solver, 32 batch-size, and 100 training epochs.

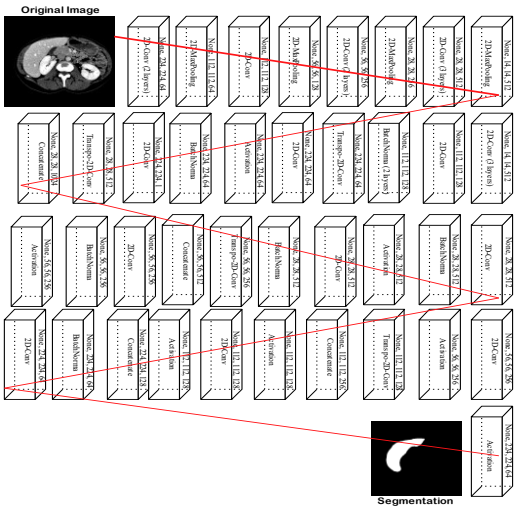

Fig. 1. Proposed semantic segmentation model.

A. Noise Reduction

Local Laplacian filters (LPF) is an operator of edge-aware where the output of the image O is defined by constructing {L[O]} coefficient [33]. The coefficient computation is independent of others. The Laplacian coefficient $L_\ell[O](x,y)$ is used to estimate the ℓ level and (x,y) position. Finally, (ℓ,x,y) coefficient of the pyramid is utilized as the value output of $L_\ell[O](x,y)$. First, the original image performed point-wise non-linearity r (.), which relies upon $g = G_\ell[I](x,y)$ pyramid of Gaussian coefficient at ℓ level and position (x,y). For example, when to maximize the detail information, S local U-shaped curve on g centered that makes values of I near to the g farther from it leaves distant unchanged values. The results are combined on different values of g and achieve the outcome. The LPF is applied on the CT slices as presented in Figure 2.

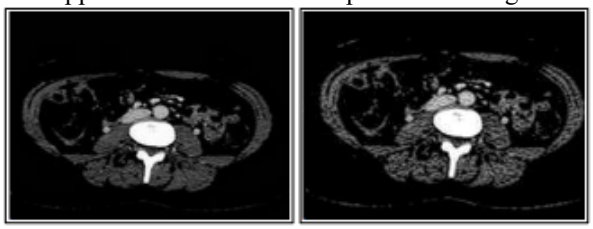

(a) (b)

Fig. 2. Results of the LPF (a) original CT slice (b) noise reduction.

The LPF parameters are depicted in Table 1.

Table I
Parameters of LPF

Symbol	Values
Σ	0.2
α	0.2

Table 1 depicts the LPF parameters in which Σ=0.2, $\alpha = 0.2$ values are selected after extensive experiments that provide better results for noise reduction.

B. Proposed Semantic Segmentation Model

In the proposed model features are extracted from VGG-16 [34] and passed input to the U-net model [35] as visualized in the Figure 3. The U-shaped network consists of encoder/decoder network. The network depth computes the time of the downsampled/upsampled input image for processing. The encoder net down samples input through 2^D factor, D denotes the depth of the encoder module. The decoder module up-sampled the encoder module output through 2^D factor.

$$\text{height} - \sum_{i=1}^{D} 2^i(c_h - 1) \quad (1)$$

$$\text{width} - \sum_{i=1}^{D} 2^i(c_w - 1) \quad (2)$$

Here c_h and c_w present height/width of 2D-Conv kernel and D=3 depth of encoder.

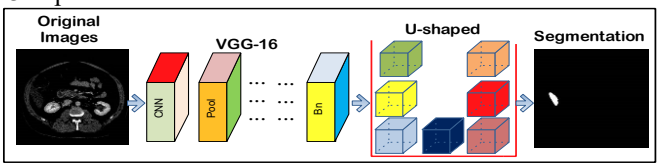

Fig. 3. Proposed steps of the segmentation model.

The proposed VGG-16-U-Shaped model contains 51 layers, such as 23 convolutional, 4 max pooling, 4 transposes convolutional, 4 concatenated, 8 activations, and 7 batch-normalization as mentioned in Table 2.

Table II
Structure of VGG-16-U-Shaped model

InputLayer	None, 224, 224, 3	Transpo-2D-Conv	None, 28, 28, 512
2D-Conv	None, 224, 224, 64	Concatenate	None, 28, 28, 1024
2D-Conv	None, 224, 224, 64	2D-Conv	None, 28, 28, 512
2D-MaxPooling	None, 112, 112, 64	BatchNorma	None, 28, 28, 512
2D-Conv	None, 112, 112, 128	Activation	None, 28, 28, 512
2D-MaxPooling	None, 56, 56, 128	2D-Conv	None, 28, 28, 512
2D-Conv	None, 56, 56, 256	BatchNorma	None, 28, 28, 512
2D-Conv	None, 56, 56, 256	Transpo-2D-Conv	None, 56, 56, 256
2D-MaxPooling	None, 28, 28, 256	Concatenate	None, 56, 56, 512
2D-Conv	None, 28, 28, 512	2D-Conv	None, 56, 56, 256
2D-Conv	None, 28, 28, 512	BatchNorma	None, 56, 56, 256
2D-Conv	None, 28, 28, 512	Activation	None, 56, 56, 256
2D-MaxPooling	None, 14, 14, 512	2D-Conv	None, 56, 56, 256
2D-Conv	None, 14, 14, 512	Activation	None, 56, 56, 256
2D-Conv	None, 14, 14, 512	Transpo-2D-Conv	None, 112, 112, 128
2D-Conv	None, 14, 14, 512	Concatenate	None, 112, 112, 256
2D-Conv	None, 112, 112, 128	Activation	None, 112, 112, 128
BatchNorma	None, 112, 112, 128	2D-Conv	None, 112, 112, 128
BatchNorma	None, 112, 112, 128	Activation	None, 112, 112, 128
Transpo-2D-Conv	None, 224, 224, 64	Concatenate	None, 224, 224,

			128
2D-Conv	None, 224, 224, 64	BatchNorma	None, 224, 224, 64
Activation	None, 224, 224, 64	2D-Conv	None, 224, 224, 64
BatchNorma	None, 224, 224, 64	Activation	None, 224, 224, 64
2D-Conv	None, 224, 224, 1		

Table 3 presents the hyperparameters of proposed VGG-16-U-Shaped model.

Table II
Hyperparameters of the proposed VGG-16-U-Shaped model

Optimizer solver	Sgdm
Epochs	100
Batch size	32

Table 3 depicts the hyperparameters that are used for model training which provide accurate outcomes for segmentation.

IV. Results

The proposed method segmentation results are validated using 3D-IRCADb and LiTS datasets. The liver segmentation is performed using FCN, SegNet, U-net and VGG-16-U-net models in term of average accuracy, loss rate and dice score.

A. Experiment Design

The proposed method results are evaluated on two publicly benchmark datasets such as 3D-IRCADb [36] and LiTS [37]. The LiTS17 dataset contains 131 cases of CT images having 512×512. 3D-IRCADb has 20 cases of which 10 are female and 10 are male. In this dataset 1353 training images with the corresponding binary masks are included.
The segmentation of liver and liver tumor results are computed numerically in term of accuracy and DSC.

$$\text{Accuracy} = \frac{\propto + \partial}{\propto + \partial + \tau + \omega}$$

$$\text{DSC} = \frac{2(a \cap b)}{a + b}$$

Where $\propto$, ∂, τ, ω denotes true positive/negative and false positive/negative respectively. The achieved segmentation results are also visually shown with ground masks.

The experiment is performed on Python, Jupyter Notebook, CORE-I7, Nvidia Graphic Card with 2071 RTX GPU, windows 11, operating system.

B. Experiment 1: Segmentation of the Liver and Liver Tumor

In this experiment, the performance of the segmentation method is accessed using different measures such as IoU, dice score, and accuracy. The graphical presentation of the presented model performance is visualized in Figure 4.

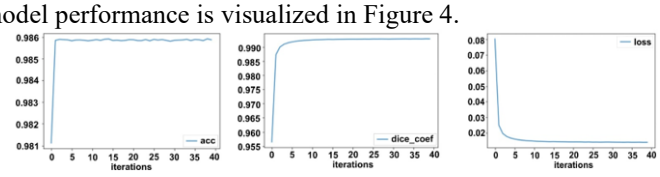

(a) (b) (c)
Fig. 4. Graphical presentation of results (a) accuracy (b) dice (c) loss rate.

In this research FCN [38], SegNet [39], U-network, and proposed method results are implemented to compute the segmentation results in different iterations as depicted in Table 4.

Table IV
Segmentation of liver in terms of dice using 3D-IRCADb

Iterations	FCN	SegNet	U-net	VGG-16-U-Shaped
1-20	0.80	0.79	0.89	0.92
21-40	0.82	0.78	0.90	0.98
41-60	0.83	0.77	0.88	0.98
61-80	0.81	0.70	0.80	0.99
81-100	0.85	0.76	0.86	0.99
101-120	0.86	0.73	0.85	0.99
121-140	0.85	0.71	0.92	0.99
141-160	0.87	0.78	0.91	0.99
161-180	0.84	0.75	0.90	0.99
181-200	0.87	0.71	0.89	0.99

In Table 4 segmentation of the liver is computed using FCN, SegNet, U-net, and the proposed VGG-16-U-Shaped model. In this experiment, we achieved maximum dice score of 0.87 on FCN, 0.79 on SegNet, 0.92 on U-net, and 0.99 on the proposed segmentation model. The outcomes demonstrate that the proposed model accurately segments the liver as compared to traditional segmentation models. The proposed segmentation model results are also compared to the existing segmentation model for segmentation of the liver tumor in Table 5.

Table V
Segmentation of liver tumor in term of dice using 3D-IRCADb

Iterations	FCN	SegNet	U-net	VGG-16-U-Shaped
1-20	0.70	0.75	0.88	0.90
21-40	0.83	0.72	0.93	0.97
41-60	0.81	0.79	0.87	0.96
61-80	0.82	0.71	0.89	0.98
81-100	0.87	0.73	0.84	0.95
101-120	0.89	0.79	0.82	0.94
121-140	0.82	0.75	0.90	0.93
141-160	0.81	0.78	0.89	0.92
161-180	0.86	0.72	0.88	0.91
181-200	0.89	0.79	0.84	0.97

In Table 5, segmentation of liver tumor results are presented in which we achieved maximum dice score of 0.89 on FCN, 0.79 on SegNet, 0.93 on U-net, and 0.98 on segmentation of the liver tumor.

The proposed segmentation outcomes on the LiTS17 dataset are mentioned in Table 6.

Table VI
Results of segmentation of liver in terms of dice using LiTS17

Iterations	FCN	SegNet	U-net	Proposed Shaped	VGG-16-U-
1-20	0.79	0.78	0.88	0.91	
21-40	0.80	0.77	0.89	0.99	
41-60	0.81	0.73	0.87	0.98	
61-80	0.80	0.72	0.85	0.95	
81-100	0.84	0.71	0.84	0.93	
101-120	0.83	0.70	0.83	0.96	
121-140	0.82	0.73	0.91	0.96	
141-160	0.86	0.76	0.90	0.99	
161-180	0.82	0.77	0.89	0.92	
181-200	0.85	0.78	0.82	0.94	

Table 6 depicts the segmentation of the liver based on LiTS17 dataset results in which we achieved a maximum dice score of 0.86 on FCN, 0.78 on SegNet, 0.91 on U-net, and 0.99 on the Proposed VGG16-U-Shaped model. Table 7 presents the segmentation of liver tumor outcomes on the LiTS17 dataset.

Table VII
Segmentation of liver tumor results on LiTS17 dataset

Iterations	FCN	SegNet	U-net	VGG-16-U-Shaped
1-20	0.68	0.74	0.87	0.92
21-40	0.81	0.71	0.91	0.95
41-60	0.79	0.78	0.85	0.98
61-80	0.79	0.73	0.88	0.99
81-100	0.76	0.75	0.83	0.92
101-120	0.74	0.77	0.81	0.95
121-140	0.73	0.78	0.89	0.96
141-160	0.76	0.79	0.82	0.97
161-180	0.81	0.71	0.86	0.98
181-200	0.85	0.76	0.83	0.99

Table 7 depicts the liver tumor segmentation on the LiTS17 dataset in which the proposed VGG-16-U-Shaped model performed better compared to FCN, SegNet, and U-net models. The segmentation results are also computed in terms of binary accuracy concerning loss rate on benchmark datasets mentioned in Tables 8 and 9.

Table VIII
roposed method results of segmentation in terms o
f loss rate and accuracy based on 3D-IRCADb

Loss rate	**Binary Accuracy**
0.1388	0.9701
0.0271	0.9861
0.0200	0.9863
0.0186	0.9853
0.0171	0.9858
0.0165	0.9855
0.0160	0.9856
0.0154	0.9859
0.0149	0.9861
0.0152	0.9856
Average Accuracy	**0.98±0.004**

Table 8 depicts the segmentation outcomes, in which the proposed method performance is validated on 100 slices of CT in terms of binary accuracy and loss rate. The achieved average accuracy is 0.98±0.004. Figure 5 depicts the segmentation results.

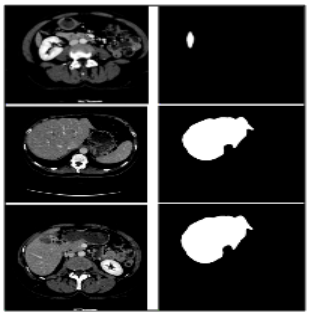

(a) (b)

Fig. 5. Outcomes of segmentation (a) original CT images (b) segmented region.

Segmentation outcomes using the 3D-IRCADb dataset are mentioned in Table 9.

Table IX
Proposed method results of liver tumor segmentation in terms of loss rate and accuracy based on LiTS17

Loss rate	Binary Accuracy
0.1289	0.9801
0.0108	0.9961
0.021	0.9753
0.0159	0.9883
0.0181	0.9808
0.0138	0.9842
0.018	0.9815
0.0163	0.9810
0.0183	0.9820
0.0149	0.9810
Average accuracy	0.9846

Table 9 depicts the segmentation method performance on CT of the LiTS17 dataset. In this experiment achieved average accuracy is 0.9846. The proposed method segmentation results are also mapped on the original images, as presented in Figure 6.

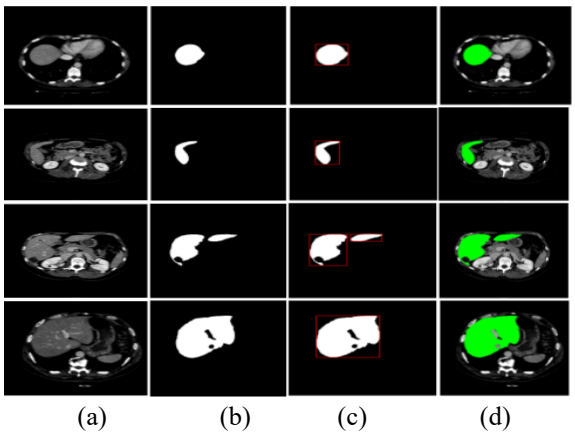

(a) (b) (c) (d)

Fig. 6. Segmentation results (a) original CT slice (b) segmentation (c) localization (d) mapped segmentation outcomes on input image.

B. Liver Segmentation Results Comparison

Table 10 presents the proposed segmentation method results in comparison.

Table X
Proposed segmentation results in comparison to the existing methods

Ref	Years	Datasets	Methods	Results (Dice)
[7]	2022	3DIRCADb	3D U-Net, superpixel, SVM	0.71 ± 0.07
[40]	2021	3DIRCADb	Encoder and decoder CNN model	0.65
[17]	2022	LiTS-2017	Pyramid decoupled co rrelation model	0.96
[41]	2022	LiTS-2017	Unet, GAN, GLCM	0.67
[42]	2022	3DIRCAD LiTS-2017	Hybrid residual model	0.72
[20]	2022	3DIRCAD LiTS-2017	HFRU-Net	0.61
[43]	2021	3Dircadb	Graph cut, region growing, and adaptive region	0.85 ± 0.05
Proposed Model		3DIRCADb	VGG-16-U-Shaped	0.99
		LiTS-2017	model	0.98

Table 10 contrasts the findings of the proposed method with existing techniques, including [7] [40] [17] [41] [42] [20] [43]. The three-dimensional U-net model is used with superpixel SLIC and SVM to segment the 3DIRCADb dataset with 0.71 ± 0.07 dice score [7]. The CNN model based on an encoder and decoder is presented for segmentation with 0.65 dice [40]. The pyramid decoupled correlation model is used to detect liver tumors, providing 0.96 dice [17]. The U-net-based generator and discriminator model are employed with GLCM for liver tumor detection. This method is tested on the LiTS-2017 dataset with 0.67 dice scores. The hybrid residual model provides 0.72 dice for liver tumor [42]. The HFRU-Net is designed and validated on 3DIRCADb and LiTS-2017 datasets that provide a global DSC of 0.61 [20]. The graph cut, region growing, and adaptive region methods are used for segmentation. The results are computed on the 3Dircadb dataset, and it provides a 0.85 ± 0.05 dice score [43].

Compared to existing works, the method proposed for liver segmentation consists of Local Laplacian Filter to improve the image quality, and Vgg-16 is used with U-net, which is trained on the selected hyperparameters to segment the tumor more accurately.

V. Conclusion

Segmentation of the liver is challenging because of its irregular structure and fuzzy boundaries. Therefore, in this research semantic segmentation model is proposed by the combination of VGG16 and U-network. The proposed segmentation network is trained on selected hyperparameters that provide more precise segmentation results. The proposed segmentation approach performance is calculated on two datasets such as 3DIRCADb and LiTS-2017. On the 3DIRCADb dataset, the proposed method provides a 0.99 dice score on the liver and 0.98 on liver tumor segmentation. Similarly, the LiTS-2017 proposed method gives a 0.97 dice score on the liver and 0.98 on the liver tumor. Compared to the current existing works, the proposed method performed better.

VI. Future Work

This work can be deployed in hospitals, and the results can benefit the radiologists' time analysis and diagnostic accuracy at an early stage to save the time and cost of treatment. In addition, the proposed method segments the 2D tumor region. Future research work might be extended/improved for tumor 3D liver segmentation.

VII. Abbreviations

All abbreviations used in this work can be indentified in table 11.

Table XI
Abbreviations Table

FCN	Fully Convolutional Neural Network
CT	Computed Tomography
LI-SLIC	Local information based SLIC
SVM	Support Vector Machine
LSTM	Long Short-Term Memory
DL	Deep Learning
SAA	Scale Attention Axis
DSC	Dice Similarity Coefficient
3D-IRCADb	3D Image Reconstruction for Comparison of Algorithm Database
VOE	Volumetric Overlap Error
MICCAI	Medical Image Computing and Computer-Assisted Intervention
AdaBoost	Adaptive Boosting
LPF	Local Laplacian Filter
GLCM	Gray-Level Co-Occurrence Matrix
HFRU-Net	High-Level Feature Fusion and Recalibration UNet
SLIC	Simple Linear Iterative Clustering

References

[1] Understanding Liver Cancer, https://www.webmd.com/cancer/understanding-liver-cancer-basic-information, Accessed by 15/8/2022.

[2] J. Amin, M. A. Anjum, M. Sharif, S. Kadry, A. Nadeem, and S. F. Ahmad, "Liver Tumor Localization Based on YOLOv3 and 3D-Semantic Segmentation Using Deep Neural Networks," *Diagnostics*, vol. 12, p. 823, 2022.

[3] C. Mattiuzzi and G. Lippi, "Cancer statistics: a comparison between world health organization (WHO) and global burden of disease (GBD)," *European journal of public health*, vol. 30, pp. 1026-1027, 2020.

[4] A. Krishan and D. Mittal, "Effective segmentation and classification of tumor on liver MRI and CT images using multi-kernel K-means clustering," *Biomedical Engineering/Biomedizinische Technik*, vol. 65, pp. 301-313, 2020.

[5] C. Zhang, J. Lu, Q. Hua, C. Li, and P. Wang, "SAA-Net: U-shaped network with Scale-Axis-Attention for liver tumor segmentation," *Biomedical Signal Processing and Control*, vol. 73, p. 103460, 2022.

[6] A. Hänsch, G. Chlebus, H. Meine, F. Thielke, F. Kock, T. Paulus, et al., "Improving automatic liver tumor segmentation in late-phase MRI using multi-model training and 3D convolutional neural networks," *Scientific Reports*, vol. 12, pp. 1-10, 2022.

[7] S. Di, Y. Zhao, M. Liao, Z. Yang, and Y. Zeng, "Automatic liver tumor segmentation from CT images using hierarchical iterative superpixels and local statistical features," *Expert Systems with Applications*, vol. 203, p. 117347, 2022.

[8] D. S. Uplaonkar and N. Patil, "Modified Otsu thresholding based level set and local directional ternary pattern technique for liver tumor segmentation," *International Journal of System Assurance Engineering and Managemen*t, pp. 1-11, 2022.

[9] H. Rahman, T. F. N. Bukht, A. Imran, J. Tariq, S. Tu, and A. Alzahrani, "A Deep Learning Approach for Liver and Tumor Segmentation in CT Images Using ResUNet," *Bioengineering*, vol. 9, p. 368, 2022.

[10] R. Zheng, Q. Wang, S. Lv, C. Li, C. Wang, W. Chen, et al., "Automatic Liver Tumor Segmentation on Dynamic Contrast Enhanced MRI Using 4D Information: Deep Learning Model Based on 3D Convolution and Convolutional LSTM," *IEEE Transactions on Medical Imaging*, 2022.

[11] J. Zhang, S. Luo, Y. Qiang, Y. Tian, X. Xiao, K. Li, et al., "Edge Constraint and Location Mapping for Liver Tumor Segmentation from Nonenhanced Images," *Computational and Mathematical Methods in Medicine*, vol. 2022, 2022.

[12] S. Gul, M. S. Khan, A. Bibi, A. Khandakar, M. A. Ayari, and M. E. Chowdhury, "Deep learning techniques for liver and liver tumor segmentation: A review," *Computers in Biology and Medicine*, p. 105620, 2022.

[13] Y. Wu, H. Shen, Y. Tan, and Y. Shi, "Automatic liver tumor segmentation used the cascade multi-scale attention architecture method based on 3D U-Net," *International Journal of Computer Assisted Radiology and Surgery*, pp. 1-8, 2022.

[14] J. Amin, M. Sharif, G. A. Mallah, and S. Fernandes, "An Optimized Features Selection Approach based on Manta Ray Foraging Optimization (MRFO) Method for Parasite Malaria Classification," *Frontiers in Public Health*, p. 2846.

[15] J. Amin, M. Sharif, M. A. Anjum, A. Siddiqa, S. Kadry, Y. Nam, et al., "3d semantic deep learning networks for leukemia detection," 2021.

[16] J. Amin, M. Sharif, M. A. Anjum, Y. Nam, S. Kadry, and D. Taniar, "Diagnosis of COVID-19 infection using three-dimensional semantic segmentation and classification of computed tomography images," *Computers, Materials and Continua*, vol. 68, pp. 2451-2467, 2021.

[17] Y. Zhang, J. Yang, Y. Liu, J. Tian, S. Wang, C. Zhong, et al., "Decoupled pyramid correlation network for liver tumor segmentation from CT images," *Medical Physics*, 2022.

[18] J. Amin, M. Sharif, and M. Almas Anjum, "Skin Lesion Detection Using Recent Machine Learning Approaches," *in Prognostic Models in Healthcare: AI and Statistical Approaches*, ed: Springer, 2022, pp. 193-211.

[19] U. Yunus, J. Amin, M. Sharif, M. Yasmin, S. Kadry, and S. Krishnamoorthy, "Recognition of Knee Osteoarthritis (KOA) Using YOLOv2 and Classification Based on Convolutional Neural Network," Life, vol. 12, p. 1126, 2022.

[20] D. T. Kushnure and S. N. Talbar, "HFRU-Net: High-level feature fusion and recalibration unet for automatic liver and tumor segmentation in CT images," *Computer Methods and Programs in Biomedicine*, vol. 213, p. 106501, 2022.

[21] H. Seo, C. Huang, M. Bassenne, R. Xiao, and L. Xing, "Modified U-Net (mU-Net) with incorporation of object-dependent high level features for improved liver and liver-tumor segmentation in CT images," *IEEE transactions on medical imaging*, vol. 39, pp. 1316-1325, 2019.

[22] C. Sun, S. Guo, H. Zhang, J. Li, M. Chen, S. Ma, et al., "Automatic segmentation of liver tumors from multiphase contrast-enhanced CT images based on FCNs," *Artificial intelligence in medicine*, vol. 83, pp. 58-66, 2017.

[23] X. Li, H. Chen, X. Qi, Q. Dou, C.-W. Fu, and P.-A. Heng, "H-DenseUNet: hybrid densely connected UNet for liver and tumor segmentation from CT volumes," *IEEE transactions on medical imaging*, vol. 37, pp. 2663-2674, 2018.

[24] K. Xia, H. Yin, P. Qian, Y. Jiang, and S. Wang, "Liver semantic segmentation algorithm based on improved deep adversarial networks in combination of weighted loss function on abdominal CT images," *IEEE Access*, vol. 7, pp. 96349-96358, 2019.

[25] J. Chi, X. Han, C. Wu, H. Wang, and P. Ji, "X-Net: Multi-branch UNet-like network for liver and tumor segmentation from 3D abdominal CT scans," *Neurocomputing*, vol. 459, pp. 81-96, 2021.

[26] Y. Tang, Y. Tang, Y. Zhu, J. Xiao, and R. M. Summers, "E $$^ $$ Net: An Edge Enhanced Network for Accurate Liver and Tumor Segmentation on CT Scans," *in International Conference on Medical Image Computing and Computer-Assisted Intervention*, 2020, pp. 512-522.

[27] W. Li, "Automatic segmentation of liver tumor in CT images with deep convolutional neural networks," *Journal of Computer and Communications*, vol. 3, p. 146, 2015.

[28] J. Zhang, Y. Xie, P. Zhang, H. Chen, Y. Xia, and C. Shen, "Light-Weight Hybrid Convolutional Network for Liver Tumor Segmentation," in IJCAI, 2019, pp. 4271-4277.

[29] H. Jiang, T. Shi, Z. Bai, and L. Huang, "Ahcnet: An application of attention mechanism and hybrid connection for liver tumor segmentation in ct volumes," *IEEE Access*, vol. 7, pp. 24898-24909, 2019.

[30] J. Stawiaski, E. Decenciere, and F. Bidault, "Interactive liver tumor segmentation using graph-cuts and watershed," in Workshop on 3D segmentation in the clinic: a grand challenge II. Liver tumor segmentation challenge. MICCAI, New York, USA, 2008.

[31] G. Chlebus, H. Meine, J. H. Moltz, and A. Schenk, "Neural network-based automatic liver tumor segmentation with random forest-based candidate filtering," arXiv preprint arXiv:1706.00842, 2017.

[32] S.-T. Tran, C.-H. Cheng, and D.-G. Liu, "A multiple layer U-Net, U n-Net, for liver and liver tumor segmentation in CT," *IEEE Access*, vol. 9, pp. 3752-3764, 2020.

[33] M. Aubry, S. Paris, S. W. Hasinoff, J. Kautz, and F. Durand, "Fast local laplacian filters: Theory and applications," *ACM Transactions on Graphics* (TOG), vol. 33, pp. 1-14, 2014.

[34] O. Russakovsky, J. Deng, H. Su, J. Krause, S. Satheesh, S. Ma, et al., "Imagenet large scale visual recognition challenge," *International journal of computer vision*, vol. 115, pp. 211-252, 2015.

[35] O. Ronneberger, P. Fischer, and T. Brox, "U-net: Convolutional networks for biomedical image segmentation," *in International Conference on Medical image computing and computer-assisted intervention*, 2015, pp. 234-241.

[36] P. F. Christ, M. E. A. Elshaer, F. Ettlinger, S. Tatavarty, M. Bickel, P. Bilic, et al., "Automatic liver and lesion segmentation in CT using cascaded fully convolutional neural networks and 3D conditional random fields," *in International conference on medical image computing and computer-assisted intervention*, 2016, pp. 415-423.

[37] C. Zhang, Q. Hua, Y. Chu, and P. Wang, "Liver tumor segmentation using 2.5 D UV-Net with multi-scale convolution," *Computers in Biology and Medicine*, vol. 133, p. 104424, 2021.

[38] J. Long, E. Shelhamer, and T. Darrell, "Fully convolutional networks for semantic segmentation," *in Proceedings of the IEEE conference on computer vision and pattern recognition*, 2015, pp. 3431-3440.

[39] K. He, X. Zhang, S. Ren, and J. Sun, "Delving deep into rectifiers: Surpassing human-level performance on imagenet classification," *in Proceedings of the IEEE international conference on computer vision*, 2015, pp. 1026-1034.

[40] B. M. Tummala and S. S. Barpanda, "Liver tumor segmentation from computed tomography images using multiscale residual dilated encoder-decoder network," *International Journal of Imaging Systems and Technology*, vol. 32, pp. 600-613, 2022.

[41] Y. Liu, F. Yang, and Y. Yang, "Free-form Lesion Synthesis Using a Partial Convolution Generative Adversarial Network for Enhanced Deep Learning Liver Tumor Segmentation," arXiv preprint arXiv:2206.09065, 2022.

[42] R. Bi, C. Ji, Z. Yang, M. Qiao, P. Lv, and H. Wang, "Residual based attention-Unet combing DAC and RMP modules for automatic liver tumor segmentation in CT," *Mathematical Biosciences and Engineering*, vol. 19, pp. 4703-4718, 2022.

[43] Z. Yang, Y.-q. Zhao, M. Liao, S.-h. Di, and Y.-z. Zeng, "Semi-automatic liver tumor segmentation with adaptive region growing and graph cuts," *Biomedical Signal Processing and Control*, vol. 68, p. 102670, 2021G. O. Young, "Synthetic structure of industrial plastics," in *Plastics,* 2nd ed., vol. 3, J . Peters, E d . New Y o r k , NY, USA: McGraw-Hill, 1964, pp. 15–64.

[44] Nie, Yali, Paolo Sommella, Marco Carratù, Mattias O'Nils, and Jan Lundgren. "A Deep CNN Transformer Hybrid Model for Skin Lesion Classification of Dermoscopic Images Using Focal Loss." *Diagnostic*s 13, no. 1 (2022): 72.

[45] Hassan, Loay, Adel Saleh, Mohamed Abdel-Nasser, Osama A. Omer, and Domenec Puig. "Promising deep semantic nuclei segmentation models for multi-institutional histopathology images of different organs." (2021).

[46] A Laishram, K Thongam, Automatic Classification of Oral Pathologies Using Orthopantomogram Radiography Images Based on Convolutional Neural Network, International Journal of Interactive Multimedia and Artificial Intelligence 7(4), pp.69-77, 2022

[47] Khattak, Muhammad Irfan, Mu'ath Al-Hasan, Atif Jan, Nasir Saleem, Elena Verdu, and Numan Khurshid. "Automated detection of COVID-19 using chest x-ray images and CT scans through multilayer-spatial convolutional neural networks." (2021).

Javeria Amin currently serves as an Assistant Professor in the Department of Computer Science, University of Wah. She is a computer vision expert. Her research focuses on anomaly detection in various parts of the human body with the help of machine learning, deep learning, and quantum computing algorithms. She is also the chief Editor of UWCS Journal and guest editor and reviewer for numerous well-reputed computer science journals. Her research work published in different international journals have a cumulative impact factor of 200+ with over 1000 citations.

Muhammad Almas Anjum is currently serving as Dean of University at National University of Technology (NUTECH), Pakistan. His areas of specialization are pattern recognition, security systems (biometrics), and computer vision. Apart of his more than 100 international publications in his area of specialization, he is the author of a book titled Face Recognition a Challenge in Biometrics: Image Resolution Issues in Face Recognition. He led the team for establishing Center of Excellence Information Technology, College of Electrical & Mechanical Engineering, and has served as its first pioneer head. He also designed and established a Center of Innovation and Entrepreneurship, College of Electrical and Mechanical Engineering. He has also served as the Dean for the Faculty of Computer Sciences, University of Wah, and the Director of Research and Development for the College of Electrical and Mechanical Engineering, NUST.

Muhammad Sharif, Ph.D. (Senior Member IEEE) is Associate Professor at COMSATS University Islamabad, Wah Campus Pakistan. He worked for one year in Alpha Soft UK-based software house in 1995. He is OCP in the Developer Track. He is in the teaching profession since 1996 to date. His research interests are Medical Imaging, Biometrics, Computer Vision, Machine Learning, and Agriculture Plants. He is being awarded COMSATS Research Productivity Award from 2011-2017. He served in TPC for IEEE FIT 2014-19 and currently serving as Associate Editor for IEEE Access, Guest Editor of Special Issues, and reviewer for well-reputed journals. He also headed the department from 2008 to 2011 and achieved the targeted outputs. He has more than 285+ research publications in IF, SCI, and ISI journals as well as in national and international conferences, and obtained 550+ Impact Factor. He has supervised/co-supervised 10 Ph.D. (CS) and 90+ MS (CS) theses to date.

Seifedine Kadry received the bachelor's degree from Lebanese University, in 1999, the M.S. degree from the University of Reims, France, and the EPFL, Lausanne, in 2002, the Ph.D. degree from Blaise Pascal University, France, in 2007, and the H.D.R. degree from the University of Rouen Normandy, in 2017. He is currently a Full Professor of data science with the Noroff University College, Norway. He is also an ABET Program Evaluator of computing and an ABET Program Evaluator of engineering technology. His current research interests include data science, education using technology, system prognostics, stochastic systems, and probability and reliability analysis.

Rubén González Crespo is a full professor in Computer Science and Artificial Intelligence. Currently he is Vice-Rector of Academic Affairs in the Universidad Internacional de La Rioja. He is also EiC and associate editor in several indexed journals. His main research areas are Artificial Intelligence, Accessibility and Project Management. He has published more than 250 scientific publications and managed several research projects. He is an advisory board member for the Ministry of Education in Colombia and Spain Mr. Author's awards and honors include the Frew Fellowship (Australian Academy of Science), the I. I. Rabi Prize (APS), the European Frequency and Time Forum Award, the Carl Zeiss Research Award, the William F. Meggers Award and the Adolph Lomb Medal (OSA).